

Influence of Solvent on Aromatic Interactions in Metal Tris-Bipyridine Complexes

Gloria A. Breault,[†] Christopher A. Hunter,^{*,‡} and Paul C. Mayers[‡]

Contribution from the Krebs Institute for Biomolecular Science, Department of Chemistry, University of Sheffield, Sheffield S3 7HF, U.K., and Zeneca Pharmaceuticals, Mereside, Alderley Park, Macclesfield, Cheshire SK10 4TG, U.K.

Received November 17, 1997

Abstract: The conformational properties of a series of iron(II) and ruthenium(II) tris-bipyridine complexes have been investigated in a range of solvents. The complexes are equipped with pendant aromatic esters attached by flexible aliphatic linkers, and aromatic interactions between the edge of the bipyridine units and the face of the aromatic esters cause the complexes to fold up in solution. The extent of folding is assessed using ¹H chemical shifts and found to be strongly solvent-dependent. Strong intramolecular edge-to-face aromatic interactions leading to stable folded structures are found in both polar solvents (water and alcohols) and nonpolar solvents (chlorinated hydrocarbons), but solvents of intermediate polarity such as DMSO destabilize the folded conformation. These results indicate that the aromatic interactions are dominated by a substantial electrostatic contribution in organic solvents but are sufficiently nonpolar to take advantage of solvophobic effects in polar solvents. This solvent dependence is likely to be a characteristic feature of any molecular recognition process which involves a mixture of both polar and nonpolar interactions.

Introduction

Desolvation is an important factor in controlling molecular recognition phenomena in solution: the hydrophobic effect,¹ removal of nonpolar residues from aqueous solvent, is one of the major forces which drives protein folding;² synthetic receptors with carefully crafted cavities which are able to completely exclude solvent, and hence do not need to be desolvated for complexation to occur, show remarkably high affinities for complementary guests.³ Diederich et al. carried out a comprehensive study of the influence of solvent on the interaction of a nonpolar aromatic guest (pyrene) with a complementary nonpolar aromatic cavity.⁴ A straightforward correlation was obtained between the stability of the host–guest complex and the polarity of the solvent. The complex is very stable in polar solvents which do not compete for the binding sites and which contribute favorably to the binding free energy through solvophobic effects. As the solvent polarity decreases, the solvophobic contribution to binding decreases and competition of the solvent for binding sites on the host and guest increases. The net result is a difference of 6 orders of magnitude in the host–guest association constant.^{4c} Hamilton et al. have

studied the influence of solvent on a different host–guest system where the major interactions controlling complexation are H-bonds.⁵ In this case, the complexes are stable in nonpolar organic solvents but become less stable as the polarity of the solvent increases, and solvent molecules begin to compete for H-bond sites on the host and guest.^{6,7}

The picture which emerges from these kinds of experiments is that complexes involving nonpolar interactions are stabilized by polar solvents and complexes involving polar interactions are stabilized in nonpolar solvents. This suggests that the way in which a molecular recognition system responds to changes in solvent can be used to derive information about the nature of the interactions which stabilize it. However, most systems of interest are complex and feature a mixture of different types of noncovalent interaction. What is the role of desolvation in these cases? For example, proteins which contain a suitable mixture of polar and nonpolar interactions are able to stabilize the same folded state in both polar and nonpolar solvents.⁸ In this paper, we describe a system which shows a more complex solvent dependence and discuss the implications for the nature of the noncovalent interactions involved.

Experimental approaches to the study of noncovalent interactions in synthetic model compounds have focused on two scenarios: intermolecular interactions in host–guest systems^{4,9} and intramolecular interactions in conformationally flexible

[‡] University of Sheffield.

[†] Zeneca Pharmaceuticals.

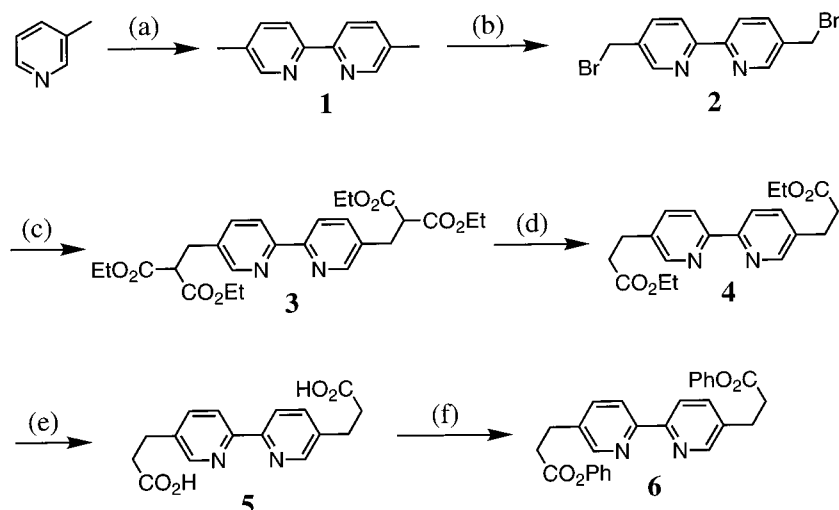
(1) (a) Hildebrand, J. H. *Proc. Natl. Acad. Sci. U.S.A.* **1979**, *76*, 194. (b) Mirejovsky, D.; Arnett, E. M. *J. Am. Chem. Soc.* **1983**, *105*, 1112. (c) Breslow, R.; Guo, T. *Proc. Natl. Acad. Sci. U.S.A.* **1990**, *87*, 167. (d) Muller, N. *Acc. Chem. Res.* **1990**, *23*, 23. (e) Dill, K. A. *Science* **1990**, *250*, 297. (f) Herzfeld, J. *Science* **1991**, *253*, 88. (g) Sharp, K. A.; Nicholls, A.; Fine, R. F.; Honig, B. *Science* **1991**, *252*, 106. (h) Nelson, J. C.; Saven, J. G.; Moore, J. S.; Wolynes, P. G. *Science* **1997**, *277*, 1793. (i) Lokey, R. S.; Iverson, B. L. *Nature* **1995**, *375*, 303–305.
(2) (a) Dill, K. A. *Biochemistry* **1990**, *29*, 7133. (b) Lins, L.; Brasseur, R. *Faseb J.* **1995**, *9*, 535.
(3) Chapman, K. T.; Still, W. C. *J. Am. Chem. Soc.* **1989**, *111*, 3075–3077.
(4) (a) Ferguson, S. B.; Sanford, E. M.; Seward, E.; Diederich, F. *J. Am. Chem. Soc.* **1991**, *113*, 5410–5419. (b) Smithrud, D. B.; Wyman, T. B.; Diederich, F. *J. Am. Chem. Soc.* **1991**, *113*, 5420–5426. (c) Smithrud, D. B.; Diederich, F. *J. Am. Chem. Soc.* **1990**, *112*, 339–343.

(5) Garcia-Tellado, F.; Goswami, S.; Chang, S. K.; Geib, S.; Hamilton, A. D. *J. Am. Chem. Soc.* **1990**, *112*, 7393.

(6) Hydrogen-bonding hosts with improved complexation properties in more polar solvents have been reported: (a) Furuta, H.; Magda, D.; Sessler, J. L. *J. Am. Chem. Soc.* **1991**, *113*, 978. (b) Kelly-Rowley, A. M.; Cabell, L. A.; Anslyn, E. V. *J. Am. Chem. Soc.* **1992**, *114*, 1900. (c) Fan, E.; Van Arman, S. A.; Kincaid, S.; Hamilton, A. D. *J. Am. Chem. Soc.* **1993**, *115*, 369.

(7) For discussions of solvent effects upon hydrogen bonding, see: Adrian, J. C.; Wilcox, C. S. *J. Am. Chem. Soc.* **1991**, *113*, 678.

(8) (a) Arakawa, T.; Goddette, D. *Arch. Biochem. Biophys.* **1985**, *240*, 21. (b) Sonnichsen, F. D.; Van Eyk, J. E.; Hodges, R. S.; Sykes, B. D. *Biochemistry* **1992**, *31*, 8790. (c) Storrs, R. W.; Truckses, D.; Wemmer, D. E. *Biopolymers* **1992**, *32*, 1695.

Scheme 1. Synthesis of Ligand 6^a

^a Reagents, conditions, and yields: (a) dehydrogenated raney nickel, reflux, 48 h (38%); (b) NBS, cat. AIBN, CCl₄, reflux, 4 h (47%); (c) (EtO₂C)₂CHLi, DMF, 50 °C, 1 h (65%); (d) wet DMSO, cat. NaCl, reflux, 2.5 h (84%); (e) NaOH, H₂O, reflux, 2 h then H₃O⁺ (90%); (f) PhOH, EDC, cat. DMAP, CH₂Cl₂, 0 °C to rt, 18 h (74%).

molecules.¹⁰ However, the limited solubility of these systems has meant that, with a few notable exceptions, the experiments have been carried out in a limited range of solvents. In this paper, we describe the properties of a new system for studying aromatic interactions based on metal tris-bipyridine complexes linked to pendant aromatic esters by flexible side chains. We demonstrate that these complexes fold up in a process driven by intramolecular aromatic interactions and that the extent to which the system is folded can be determined by changes in ¹H NMR chemical shift in a variety of solvents. The folding process is strongly solvent-dependent, and the unusual trends in stability provide new insight into the nature of the aromatic interactions involved.

Synthesis

5,5'-Dimethyl-2,2'-bipyridine (**1**) was prepared¹¹ and converted to dibromide **2**¹² following literature procedures. A modified malonate-type reaction with diethylmalonate lithium salt in DMF gave tetraester **3** in 65% yield which was

(9) Adams, H.; Harris, K. D. M.; Hembury, G. A.; Hunter, C. A.; Livingstone, D.; McCabe, J. F. *J. Chem. Soc., Chem. Commun.* **1996**, 2531–2532. (b) Adams, H.; Carver, F. J.; Hunter, C. A.; Morales, J. C.; Seward, E. M. *Angew. Chem., Int. Ed. Engl.* **1996**, *35*, 1542–1544. (c) Ferguson, S. B.; Diederich, F. *Angew. Chem., Int. Ed. Engl.* **1986**, *25*, 1127–1129. (d) Kato, Y.; Conn, M. M.; Rebek, J. *J. Am. Chem. Soc.* **1994**, *116*, 3279–3284. (e) Aoyama, Y.; Asakawa, M.; Yamagishi, A.; Toi, H.; Ogoshi, H. *J. Am. Chem. Soc.* **1990**, *112*, 3145–3151. (f) Aoyama, Y.; Asakawa, M.; Matsui, Y.; Ogoshi, H. *J. Am. Chem. Soc.* **1991**, *113*, 6233–6240. (g) Rebek, J.; Nemeth, D. *J. Am. Chem. Soc.* **1986**, *108*, 5637–5638. (h) Jeong, K. S.; Rebek, J. *J. Am. Chem. Soc.* **1988**, *110*, 3327–3328. (i) Muehldorf, A. V.; Vanengen, D.; Warner, J. C.; Hamilton, A. D. *J. Am. Chem. Soc.* **1988**, *110*, 6561–6562. (j) Zimmerman, S. C.; Vanzyl, C. M.; Hamilton, G. S. *J. Am. Chem. Soc.* **1989**, *111*, 1373–1381. (k) Zimmerman, S. C.; Kwan, W. S. *Angew. Chem., Int. Ed. Engl.* **1995**, *34*, 2404–2406. (l) Zimmerman, S. C. *Top. Curr. Chem.* **1993**, *165*, 71–102. (m) Schneider, H. *J. Angew. Chem., Int. Ed. Engl.* **1991**, *30*, 1417–1436.

(10) (a) Eliel, E. L.; Allinger, N. L.; Angyal, S. J.; Morrison, G. A. *Conformational Analysis*; Interscience: New York, 1965. (b) Gallo, E. A.; Gellman, S. H. *J. Am. Chem. Soc.* **1993**, *115*, 9774–9788. (c) Newcomb, L. F.; Haque, T. S.; Gellman, S. H. *J. Am. Chem. Soc.* **1995**, *117*, 6509–6519. (d) Newcomb, L. F.; Gellman, S. H. *J. Am. Chem. Soc.* **1994**, *116*, 4993–4994. (e) Paliwal, S.; Geib, S.; Wilcox, C. S. *J. Am. Chem. Soc.* **1994**, *116*, 4497–4498. (f) Cozzi, F.; Cinquini, M.; Annunziata, R.; Dwyer, T.; Siegel, J. S. *J. Am. Chem. Soc.* **1992**, *114*, 5729–5733. (g) Cozzi, F.; Cinquini, M.; Annunziata, R.; Siegel, J. S. *J. Am. Chem. Soc.* **1993**, *115*, 5330–5331. (h) Cozzi, F.; Ponzini, F.; Annunziata, R.; Cinquini, M.; Siegel, J. S. *Angew. Chem., Int. Ed. Engl.* **1995**, *34*, 1019–1020. (i) Cozzi, F.; Siegel, J. S. *Pure Appl. Chem.* **1995**, *67*, 683–689.

decarboxylated using the procedure of Krapcho *et al.*¹³ to give **4**¹⁴ (84%). Subsequent base hydrolysis gave the diacid **5** (90%) which was coupled with phenol using 1-(3-(dimethylamino)propyl)-3-ethylcarbodiimide hydrochloride (EDC) to give phenyl diester **6** (74%) (Scheme 1).

Iron(II) complexes of **4** and **6** were prepared quantitatively by treatment of the ligand with a solution of 0.33 equiv of the required iron salt: Fe(ClO₄)₂·6H₂O in 5% methanol/CH₂Cl₂ gave the perchlorate salts, and FeCl₂·4H₂O in methanol gave the chloride salts (Scheme 2).

The corresponding ruthenium(II) complexes were prepared by treatment of **4** with RuCl₃ in refluxing ethylene glycol, followed by base hydrolysis and ion exchange to give Ru^{II}**5**₃ (PF₆)₂ in 77% yield. EDC coupling with phenol then gave the hexaphenyl ester Ru^{II}**6**₃ (PF₆)₂ in 70% yield, and that with *n*-pentanol gave the hexapentyl ester Ru^{II}**7**₃ (PF₆)₂ (47%) (Scheme 3). Unsymmetrical ruthenium(II) complexes were prepared by treatment of **1** with RuCl₃·3H₂O and LiCl in refluxing DMF to give the *cis*-dichloride Ru^{II}**1**₂·Cl₂ (83%), and subsequent reaction with a slight excess of **4** in aqueous ethanol followed by ion exchange gave Ru^{II}**4**₁₂ (PF₆)₂ (72%).¹⁵ Base hydrolysis followed by an EDC coupling with phenol gave the diphenyl ester Ru^{II}**6**₁₂ (PF₆)₂ (72%) (Scheme 4).

Results and Discussion

Evidence for Intramolecular Aromatic Interactions. During our work with a range of tris-bipyridine metal complexes such as Fe^{II}**6**₃, Fe^{II}**4**₃, Ru^{II}**6**₃, and Ru^{II}**7**₃, we noticed that the ¹H NMR chemical shifts of protons H₃ and H₄ were very sensitive to the nature of the ester substituent on the end of the chain. For example, in chloroform the ¹H NMR signal due to H₃ is shifted 0.54 ppm upfield in Fe^{II}**6**₃ (ClO₄)₂ relative to the signal due to the same proton in Fe^{II}**4**₃ (ClO₄)₂ (Figure 1). If we compare the ¹H NMR spectra of the uncomplexed free

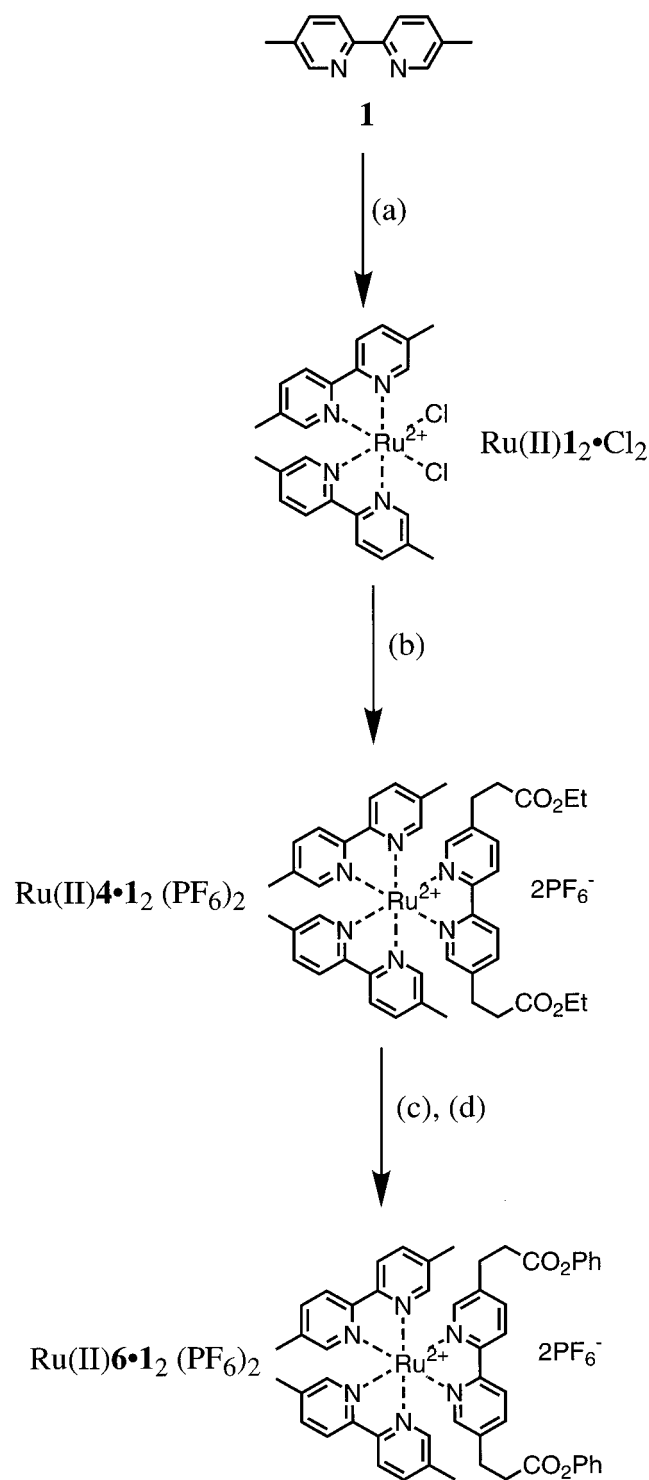
(11) (a) Sasse, W. H. F.; Whittle, C. P. *J. Chem. Soc.* **1961**, 1347–1350. (b) Badger, G. M.; Sasse, W. H. F. *J. Chem. Soc.* **1956**, 616–620.

(12) Ebmeyer, F.; Vögtle, F. *Chem. Ber.* **1989**, *122*, 1725–1727.

(13) Krapcho, A. P.; Lovey, A. J. *Tetrahedron Lett.* **1973**, 957–960.

(14) (a) Hamilton, A. D.; Rubin, H.-D.; Bocarsly, A. B. *J. Am. Chem. Soc.* **1984**, *106*, 7255–7257. (b) Hamilton, A. D. Private communication.

(15) (a) Lay, P. A.; Sargeson, A. M.; Taube, H. *Inorg. Synth.* **1986**, *24*, 291–299. (b) Sprintschnik, G.; Sprintschnik, H. W.; Kirsch, P. P.; Whitton, D. G. *J. Am. Chem. Soc.* **1977**, *99*, 4947–4954.

Scheme 4. Synthesis of Ru^{II}1₂•6 (PF₆)₂^a

^a Reagents, conditions, and yields: (a) RuCl₃•3H₂O, LiCl, DMF, reflux, 7 h (83%); (b) 1.1 equiv of **4**, 50% aq ethanol, reflux, 3 h then NH₄PF₆ (72%); (c) NaOH, water, reflux, 2.5 h then H₃O⁺/NH₄PF₆ (96%); (d) PhOH, EDC, cat. DMAP, CH₂Cl₂, 0 °C to rt, 18 h (75%).

ligands **6** and **4**, there is a 0.09 ppm downfield shift of H₃, so the very large difference observed in the metal complexes is clearly not due to through-bond effects (Figure 1).

One possibility is that the large shifts are caused by ion-pairing interactions with the counterions. However, ¹H NMR dilution studies revealed very small concentration-dependent changes in chemical shift. Typical results are shown for the signals due to proton H₃ in Ru^{II}6₃ (PF₆)₂ and Ru^{II}7₃(PF₆)₂ in

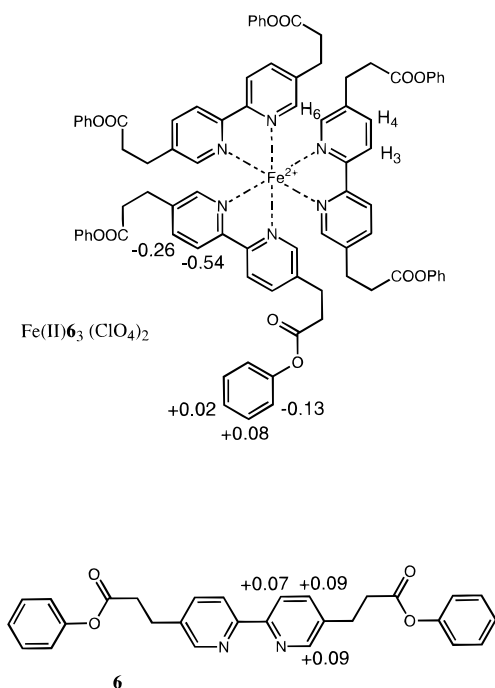


Figure 1. Chemical shift changes observed for Fe^{II}6₃ (ClO₄)₂ and free ligand **6** in chloroform. Shifts for the bipyridine protons of Fe^{II}6₃ (ClO₄)₂ are relative to those for Fe^{II}4₃ (ClO₄)₂ and the phenolic protons are relative to those of **6**. Shifts for **6** are relative to those for ethyl ester **4**.

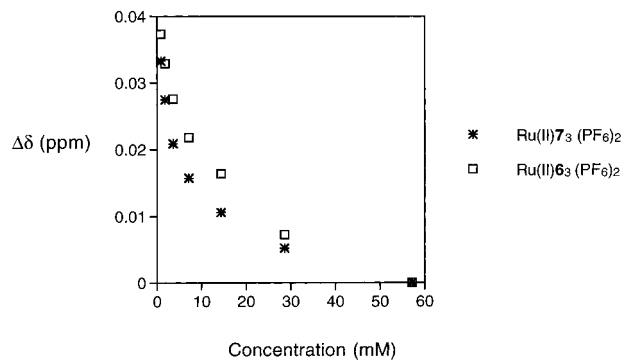


Figure 2. Variation of chemical shift of bipyridine H₃ with concentration for Ru^{II}6₃ (PF₆)₂ and Ru^{II}7₃ (PF₆)₂ in acetone-*d*₆. Δδ values are quoted relative to those obtained at the highest recorded concentration (57 mM).

acetone (Figure 2). For this system, the difference between the chemical shift of the signal due to H₃ in Ru^{II}6₃ (PF₆)₂ and the corresponding proton in the alkyl ester reference compound Ru^{II}7₃ (PF₆)₂ is -0.37 ppm. Dilution of the complexes resulted in changes in chemical shift of less than 0.05 ppm, and both complexes exhibited almost identical changes over the same concentration range. Thus the small concentration-dependent changes in chemical shift which are observed are not related to the large difference observed between the aromatic and alkyl esters. This indicates that even if ion pairing does take place to a significant extent in this system, it has a negligible effect on the observed differences in ¹H NMR chemical shift in which we are interested.

A more likely explanation of these observations is that the large shifts observed for the aromatic esters are caused by intramolecular aromatic interactions in the complex. These interactions lead to close proximity of the phenyl esters and the bipyridine groups in the metal complex which in turn causes ring current-induced changes in chemical shift. The bipyridine

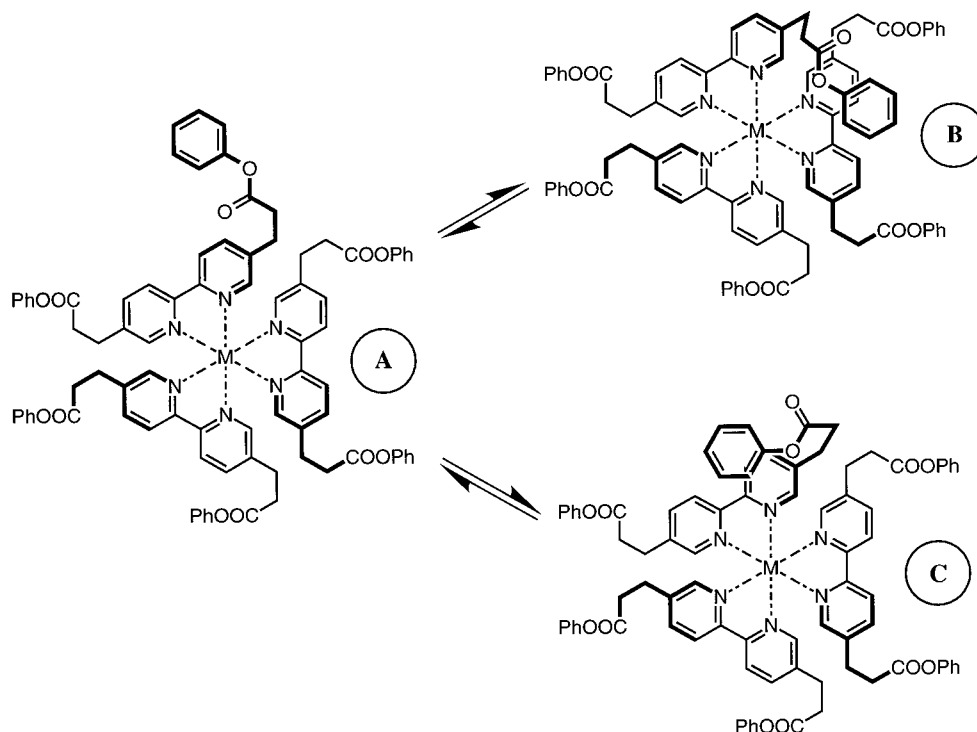


Figure 3. Conformational equilibria for tris-bipyridine complexes of type $M^{II}_3 X_2$.

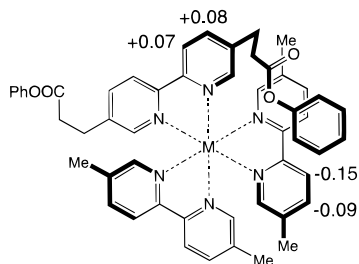


Figure 4. Chemical shift changes observed for $Ru^{II}_2 \cdot 6 (PF_6)_2$ relative to $Ru^{II}_2 \cdot 4 (PF_6)_2$ in acetone- d_6 .

protons H_3 and H_4 experience large upfield shifts in $Fe^{II}_3 (PF_6)_2$ relative to $Fe^{II}_3 (PF_6)_2$, whereas the phenyl ester protons are not significantly shifted relative to those of the free ligand **6** which implies that the bipyridine protons lie over the face of the phenyl ester rings (Figure 1). Figure 3 illustrates conformational equilibria which could explain the NMR data. In conformation A, the ester group is directed away from the complex and there are no aromatic interactions. Conformations B and C show two different types of geometry in which there is an interaction between the bipyridine protons and the face of a phenyl ester ring. Large differences in chemical shift are not observed between the uncomplexed free ligands **4** and **6** which implies that bending back of the phenyl ester onto its own bipyridine unit as in conformation C is not very probable. However, it is possible that complexation of the bipyridine by the metal cation significantly polarizes protons H_3 and H_4 which increases the electrostatic interaction of these protons with the π -electrons on the face of the phenyl ester ring. Therefore, to distinguish conformations B and C, we prepared the unsymmetrical complex $Ru^{II}_6 \cdot 1_2 (PF_6)_2$.

The differences in 1H NMR chemical shift between the bipyridine protons of $Ru^{II}_6 \cdot 1_2 (PF_6)_2$ and the corresponding alkyl ester reference compound $Ru^{II}_4 \cdot 1_2 (PF_6)_2$ in acetone are shown in Figure 4. H_3 and H_4 of the bipyridine unit containing the pendant phenyl esters (**6**) are shifted slightly downfield: the shifts are in fact very similar to the differences observed for

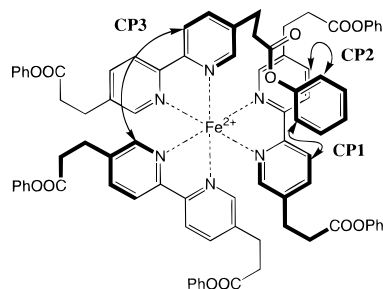


Figure 5. NOEs observed in a 400 MHz ROESY spectrum of $Fe^{II}_3 (ClO_4)_2$ in $CDCl_3$.

the uncomplexed free ligands **6** and **4**. The analogous H_3 and H_4 protons on the dimethylbipyridine units (**1**) however show significant upfield shifts (the values in Figure 4 are averaged, since the two pyridine rings of each bipyridine unit are nonequivalent but behave similarly). Correcting for the influence of metal coordination on the chemical shifts of the bipyridine protons, it is clear that there are large upfield shifts of the bipyridine protons on **1** and no shifts on **6** which proves that the aromatic interaction in this system is due to type B conformations rather than type C conformations (Figure 3). The magnitudes of the shifts observed in $Ru^{II}_6 \cdot 1_2 (PF_6)_2$ (-0.15 and -0.09 ppm) are approximately one-half those observed in $Ru^{II}_3 (PF_6)_2$ (-0.37 and -0.12 ppm), because only one phenyl ester ring can interact with each set of dimethylbipyridine protons whereas in complex $Ru^{II}_6 (PF_6)_2$ in conformation B two phenyl ester groups interact with each set of bipyridine protons.

Further evidence for the folded conformation of the aromatic esters was obtained from two-dimensional ROESY experiments. Cross-peaks connecting the signals due to the bipyridine protons H_3 and H_4 and the signal due to the *o*-phenyl ester protons (CP1 and CP2 in Figure 5) indicate that these two parts of the molecule are close in space (Figure 5). These observations are clearly consistent with the folded conformation B shown in Figure 3.

We have also investigated the conformational properties of

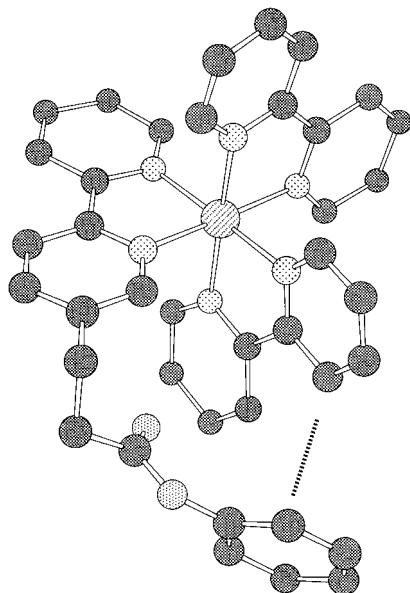


Figure 6. Typical low-energy conformation of $\text{Ru}^{\text{II}}12\cdot6$ obtained from a Monte Carlo conformational search using the Macromodel implementation of the MM2 force field with chloroform solvation.

Table 1. Temperature-Dependent Changes in Chemical Shift of $\text{Fe}^{\text{II}}6_3$ (ClO_4)₂ Relative to $\text{Fe}^{\text{II}}4_3$ (ClO_4)₂

high temperature ($\text{Cl}_2\text{DCCDCl}_2$)		low temperature (CDCl_3)	
T (K)	$\Delta\delta$ H ₃ (ppm)	T (K)	$\Delta\delta$ H ₃ (ppm)
295	-0.500	295	-0.537
313	-0.488	268	-0.568
330	-0.473	258	-0.574
346	-0.462	243	-0.593
366	-0.445	228	-0.614

^a All spectra were recorded at a concentration of 8 mM.

this system using molecular mechanics calculations. The X-ray crystal structure of ruthenium(II) tris-bipyridine was retrieved from the Cambridge Crystallographic Database and used as a starting point for molecular modeling studies.¹⁶ One phenyl ester side chain was attached, and a conformational search was carried out using the Macromodel¹⁷ implementation of the MM2 force field with chloroform solvation and constraining the ruthenium(II) tris-bipyridine core to the X-ray structure geometry. In other words, we probed the conformational properties of the flexible side chain only. Not surprisingly, a large number of different low-energy conformations were obtained. However, a number of these structures corresponded to conformation B, and none of the low-energy structures were in conformation C, which is consistent with the experimental observations. A representative type B conformation is shown in Figure 6. We do not suggest that this is the optimal or most populated conformation; it simply illustrates one of the conformations which is populated to a significant extent and which is responsible for the large ring current shifts observed in this system.

The temperature dependence of the NMR shifts was investigated for $\text{Fe}^{\text{II}}6_3$ (ClO_4)₂ and $\text{Fe}^{\text{II}}4_3$ (ClO_4)₂ in tetrachloroethane-1,1,2,2-*d*₂ (for high temperatures) and CDCl_3 (for low temperatures). The results are shown in Table 1 and Figure 7. At higher temperatures, the differences in chemical shift between

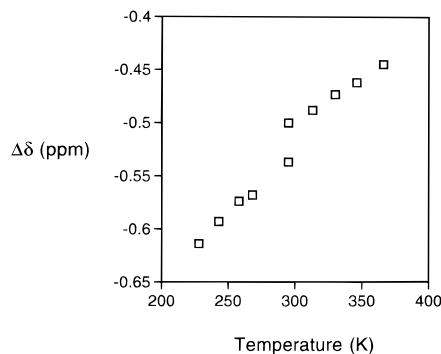


Figure 7. Variation of chemical shift with temperature for bipyridine H₃ of $\text{Fe}^{\text{II}}6_3$ (ClO_4)₂ relative to $\text{Fe}^{\text{II}}4_3$ (ClO_4)₂ in $\text{C}_2\text{D}_2\text{Cl}_4$ (≥ 295 K) and CDCl_3 (≤ 295 K). The discontinuity at 295 K is due to the change in solvent at this temperature.

Table 2. Changes in Chemical Shift of Iron(II) Complexes $\text{Fe}^{\text{II}}6_3$ (ClO_4)₂ and $\text{Fe}^{\text{II}}6_3$ Cl_2 Relative to $\text{Fe}^{\text{II}}4_3$ (ClO_4)₂ and $\text{Fe}^{\text{II}}4_3$ Cl_2 ^a

solvent	Z (kcal mol ⁻¹)	$\Delta\delta$ (ppm)			counterion
		H ₃	H ₄	H ₆	
CDCl_3	63.2	-0.54	-0.26	+0.02	ClO_4^-
CD_2Cl_2	64.2	-0.48	-0.20	<i>b</i>	ClO_4^-
acetone- <i>d</i> ₆	65.7	-0.34	-0.15	<i>b</i>	ClO_4^-
DMF- <i>d</i> ₇	68.5	-0.25	-0.07	<i>b</i>	ClO_4^-
DMSO- <i>d</i> ₆	71.1	-0.12	-0.08	+0.03	ClO_4^-
CD_3CN	71.3	-0.32	-0.12	+0.01	ClO_4^-
<i>i</i> PrOD- <i>d</i> ₇	76.3	-0.51	-0.18	<i>b</i>	Cl^-
CD_3OD	83.6	-0.56	-0.23	-0.06	Cl^-
D_2O	94.6	-0.81	-0.31	-0.09	Cl^-

^a All spectra were recorded at a concentration of 8 mM with the exception of the D_2O sample where a lower concentration (ca. 2 mM) was used due to limited solubility. ^b Values could not be obtained due to overlapping signals in $\text{Fe}^{\text{II}}6_3$.

the aromatic and alkyl esters are significantly reduced, while at low temperatures the differences increase. This is consistent with the model in Figure 3 where there is an equilibrium between a folded conformation (B) stabilized by attractive aromatic interactions and an unfolded disordered conformation (A). High temperatures shift the equilibrium toward the disordered conformation (A), and low temperatures favor the more ordered state (conformation B). It seems that the two extreme conformations illustrated in Figure 3 are never fully populated within the temperature range studied.

These experiments demonstrate that there is a strong intramolecular aromatic interaction in this system. The differences between the chemical shifts of the ¹H NMR signals due to the bipyridine protons H₃ and H₄ in the aromatic esters and the corresponding alkyl ester control compounds provide a simple measure of the position of the equilibrium between conformation A and conformation B (Figure 3) and hence a direct measure of the strength of the intramolecular aromatic interaction. The solubility of metal complexes of this type can easily be controlled by choice of counterions, so this represents an ideal system for investigating the influence of solvent on the magnitude of aromatic interactions.

Solvent Dependence of Aromatic Interactions. The perchlorate and chloride salts of the iron(II) complexes and the hexafluorophosphate salts of the ruthenium(II) complexes allowed us to record ¹H NMR spectra in a wide range of solvents. The results are summarized in Tables 2 and 3 and Figure 8. The differences in chemical shift which we use to quantify the aromatic interactions show an interesting variation with solvent polarity (quantified by the parameter Z).¹⁸ Large upfield shifts are observed in polar solvents, e.g., water, and as

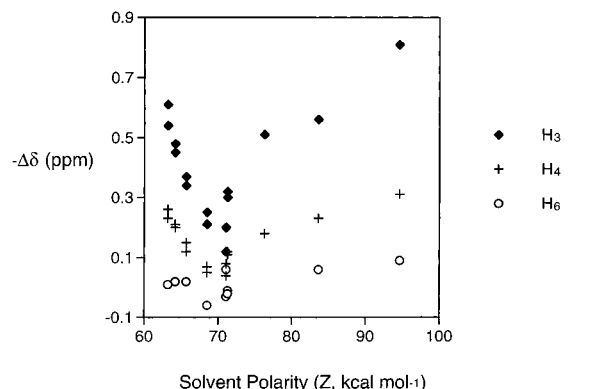
(16) Fletcher, D. A.; McMeeking, R. F.; Parkin, D. J. *J. Chem. Inf. Comput. Sci.* **1996**, *36*, 746-749.

(17) Mohamadi, F.; Richards, N. G. J.; Guida, W. C.; Liskamp, R.; Lipton, M.; Caufield, C.; Chang, G.; Hendrickson, T.; Still, W. C. *J. Comput. Chem.* **1990**, *11*, 440-467.

Table 3. Changes in Chemical Shift of Ruthenium(II) Complex $\text{Ru}^{\text{II}}\text{6}_3(\text{PF}_6)_2$ Relative to $\text{Ru}^{\text{II}}\text{7}_3(\text{PF}_6)_2^a$

solvent	Z (kcal mol ⁻¹)	$\Delta\delta$ (ppm)		
		H ₃	H ₄	H ₆
CDCl_3	63.2	-0.61	-0.23	-0.01
CD_2Cl_2	64.2	-0.45	-0.21	-0.02
acetone- <i>d</i> ₆	65.7	-0.37	-0.12	-0.02
DMF- <i>d</i> ₇	68.5	-0.21	-0.05	+0.06
DMSO- <i>d</i> ₆	71.1	-0.20	-0.04	-0.06
CD_3CN	71.3	-0.30	-0.11	+0.02

^a All spectra were recorded at a concentration of 8 mM.

**Figure 8.** Differences in chemical shift between H₃, H₄, and H₆ of $\text{Fe}^{\text{II}}\text{6}_3(\text{ClO}_4)_2$ and $\text{Ru}^{\text{II}}\text{6}_3(\text{PF}_6)_2$ and their respective reference complexes as a function of solvent polarity.

the solvent polarity decreases, the magnitude of the shift decreases. This is consistent with a solvophobic description of aromatic interactions: the interactions are strongest in polar solvents which are unable to properly solvate the nonpolar surfaces of the aromatic rings.⁴ However, as the solvent polarity decreases further, the strength of the aromatic interaction goes through a minimum at DMSO and then starts to increase again. By the time we reach chloroform, the magnitude of the interaction is comparable to that in water. This suggests that in nonpolar solvents, electrostatic interactions become dominant and lead to large attractive interactions between the aromatic rings.¹⁹

Further attempts to investigate the relative strengths of the interactions were made using 2D ROESY experiments on $\text{Fe}^{\text{II}}\text{6}_3(\text{ClO}_4)_2$ in CDCl_3 and DMSO-*d*₆ and $\text{Fe}^{\text{II}}\text{6}_3\text{Cl}_2$ in CD_3OD . A qualitative estimate of the average distance between the interacting aromatic rings was obtained by integrating the corresponding NOE cross-peaks (CP1 and CP2 in Figure 5) and normalizing the intensities relative to the H₃–H₆ cross-peak (CP3 in Figure 5): the H₃–H₆ distance is constrained by the covalent and coordination bonding in the complex and so is solvent-independent. The normalized cross-peaks labeled CP1 and CP2 in Figure 5 are significantly more intense in the CD_3OD and CDCl_3 spectra compared with the DMSO-*d*₆ spectrum. Thus the aromatic rings spend less time in close proximity in DMSO than in the other two solvents in accord with the chemical shift experiments.

Conclusions

The ¹H NMR chemical shifts of the metal tris-bipyridine complexes reported above indicate that there are strong in-

(18) Z values were obtained from Gordon, A. J.; Ford, R. A. *The Chemist's Companion*; Wiley: New York, 1972; pp 22–23 and references therein. Isotope effects for deuterated solvents were ignored. For a discussion of the derivation of Z values, see: Kosower, E. M. *J. Am. Chem. Soc.* **1958**, *80*, 3253–3270.

(19) (a) Hunter, C. A.; Sanders, J. K. M. *J. Am. Chem. Soc.* **1990**, *112*, 5525–5534. (b) Hunter, C. A. *Chem. Soc. Rev.* **1994**, *23*, 101–109.

tramolecular interactions between the pendant aromatic ester groups and the aromatic core of the complex. These interactions cause the complexes to fold up in solution, and the extent of folding is strongly solvent-dependent. However, the relationship between solvent polarity and folding (or the strength of the aromatic interactions) is not simple. The aromatic interactions are strongest in water, where there is a substantial hydrophobic contribution. As the solvent polarity decreases, the interactions decrease until we reach DMSO. Then the interactions start to become more favorable again, and by the time we reach chloroform, they are almost as strong as they are in water. This indicates that there is a substantial electrostatic contribution to the aromatic interactions which dominates in very nonpolar solvents. The bipyridine rings are strongly polarized by the metal centers in these systems, and so the electrostatic component of this interaction is likely to be much larger than in interactions between simple aromatic rings. However, the results clearly demonstrate that electrostatics are an important factor even in interactions between relatively nonpolar groups. We believe that the biphasic behavior of this system is likely to be representative of the solvent dependence of the majority of molecular recognition events which involve combinations of polar and nonpolar (or solvophobic) interactions. It is no coincidence that the solvent which lies at the bottom of the curve in Figure 8 is DMSO: it is one of the best general solvents known because it competes effectively for both polar and nonpolar interaction sites.

Experimental Section

¹H and ¹³C NMR spectra were recorded on a Bruker AC 250 or AM 250 MHz spectrometer operated in Fourier transform mode. Chemical shifts were referenced to TMS as an internal standard. All solvent-dependent measurements were made on the AM 250 instrument. 2D ROESY spectra were recorded on a Bruker AMX 400 MHz spectrometer. FAB⁺ mass spectra were recorded on a Kratos MS80 using a matrix of *m*-nitrobenzyl alcohol (NOBA) and positive electrospray spectra on a Kratos MS25. UV/visible spectra were recorded on a Phillips PU 8720 scanning spectrophotometer using quartz cuvettes in either dry CH_2Cl_2 or spectroscopic grade methanol. IR spectra were recorded on a Perkin-Elmer Paragon 1000 spectrometer, and samples were prepared as a Nujol mull. Melting points were recorded on a Reichter Kofler hot stage melting point apparatus and are uncorrected. Microanalyses were performed using a Perkin-Elmer 2400 CHN elemental analyzer working at 975 °C. Where specified, CH_2Cl_2 was dried by distillation from CaH_2 . Dry ruthenium trichloride was prepared by heating the trihydrate at 140 °C for 48 h and was assumed to have composition RuCl_3 .

Molecular modeling was carried out using the MacroModel v4.5 implementation of the MM2 force field¹⁷ with chloroform solvation. The core of the complex (metal and bipyridine rings) was constrained to the X-ray crystal structure geometry found for $\text{Ru}(\text{bipy})_3$ in the Cambridge Structure Database, and Monte Carlo searching was employed to locate local energy minimum conformations for the flexible sidearm.

5,5'-Bis(2,2-dicarbethoxyethyl)-2,2'-bipyridine (3). Lithium hydride (0.159 g, 20 mmol) was added in one portion to a solution of diethyl malonate (5.86 g, 36.6 mmol) in dimethylformamide (DMF) (10 mL) and stirred for 1 h. Solid **2** (1.00 g, 2.92 mmol) was added in one portion and stirred for 30 min at 20 °C followed by 1 h at 50 °C. Water (10 mL) was added to the mixture which was then extracted with diethyl ether (3 × 50 mL). The combined extracts were washed with water (3 × 50 mL), dried (Na_2SO_4), filtered, and evaporated to give a yellow oil from which white crystals formed overnight. The crystals were removed by filtration, washed well with petroleum ether (bp 40–60 °C), and dried in vacuo to yield the title compound (0.948 g, 65%): $R_f = 0.4$ (Et_2O); mp 123–124 °C; ¹H NMR (250 MHz, CDCl_3) δ 1.22 (12H, t, $J = 7$ Hz, $-\text{CH}_3$), 3.26 (4H, d, $J = 8$ Hz, ArCH_2-), 3.66 (2H, t, $J = 8$ Hz, $\text{ArCH}_2\text{CH}_2-$), 4.16 (8H, m, $-\text{OCH}_2-$), 7.67 (2H,

dd, $J = 8, 2$ Hz, 4-pyridine H), 8.27 (2H, d, $J = 8$ Hz, 3-pyridine H), 8.52 (2H, d, $J = 2$ Hz, 6-pyridine H); ^{13}C NMR (62.9 MHz, CDCl_3) δ 14.0, 31.7, 53.3, 61.7, 120.6, 133.5, 137.3, 149.6, 154.6, 168.4; FAB^+ MS $m/z = 501$ (100, MH^+), $\text{C}_{26}\text{H}_{32}\text{N}_2\text{O}_8$ requires 500.53; $v = 1720$ cm^{-1} ($\text{C}=\text{O}$). Calculated for $\text{C}_{26}\text{H}_{32}\text{N}_2\text{O}_8$: C, 62.39; H, 6.44; N, 5.60. Found: C, 62.41; H, 6.20; N, 5.52.

5,5'-Bis(2-carbomethoxyethyl)-2,2'-bipyridine (4). **3** (7.50 g), water (2.025 g), and sodium chloride (2.10 g) were refluxed in dimethyl sulfoxide (DMSO) (100 mL) for 2.5 h with the exclusion of light. After the mixture cooled, diethyl ether (400 mL) was added and the ether layer washed with water (5×150 mL) before being dried (Na_2SO_4) and filtered through 5 cm of silica gel. The solvent was then removed in vacuo to yield the title compound as a white crystalline solid (4.50 g, 84%): $R_f = 0.50$ (10% methanol/ CH_2Cl_2); mp 87–89 °C; ^1H NMR (250 MHz, CDCl_3) δ 1.22 (6H, t, $J = 7$ Hz, $-\text{CH}_3$), 2.55 (4H, t, $J = 8$ Hz, $-\text{CH}_2-$), 2.98 (4H, t, $J = 8$ Hz, $-\text{CH}_2-$), 4.12 (4H, q, $J = 7$ Hz, $-\text{OCH}_2-$), 7.65 (2H, dd, $J = 8, 2$ Hz, 4-pyridine H), 8.26 (2H, d, $J = 8$ Hz, 3-pyridine H), 8.52 (2H, d, $J = 2$ Hz, 6-pyridine H); ^{13}C NMR (62.9 MHz, CDCl_3) δ 14.2, 28.0, 35.4, 60.6, 120.6, 135.9, 136.8, 149.2, 154.4, 172.4; FAB^+ MS $m/z = 357$ (100, MH^+), $\text{C}_{20}\text{H}_{24}\text{N}_2\text{O}_4$ requires 356.42; $v = 1722$ cm^{-1} ($\text{C}=\text{O}$). Calculated for $\text{C}_{20}\text{H}_{24}\text{N}_2\text{O}_4$: C, 67.40; H, 6.79; N, 7.86. Found: C, 67.33; H, 6.77; N, 7.85.

5,5'-Bis(2-carboxyethyl)-2,2'-bipyridine (5). Sodium hydroxide (0.85 g, 21.25 mmol) and **4** (1.50 g, 4.208 mmol) were refluxed for 2 h in water (10 mL). After cooling and neutralization with concentrated HCl (36%, 2.15 g, 21.25 mmol), the product was removed by filtration, washed well with water and diethyl ether, and then dried in vacuo at 60 °C overnight to give the title compound as a white solid (1.13 g, 90%): $R_f = 0.0$ (15% methanol/ CH_2Cl_2); mp 246–249 °C; ^1H NMR (250 MHz, $\text{DMSO}-d_6$) δ 2.62 and 2.89 (2 \times 4H, 2t, $J = 8$ Hz, $-\text{CH}_2\text{CH}_2-$), 7.79 (2H, dd, $J = 8, 2$ Hz, 4-pyridine H), 8.27 (2H, d, $J = 8$ Hz, 3-pyridine H), 8.54 (2H, d, $J = 2$ Hz, 6-pyridine H), 12.25 (2H, br, $-\text{CO}_2\text{H}$); ^{13}C NMR (62.9 MHz, $\text{DMSO}-d_6$) δ 27.8, 35.1, 120.3, 137.1, 137.5, 149.6, 153.7, 174.0; FAB^+ MS $m/z = 301$ (100, MH^+), $\text{C}_{16}\text{H}_{16}\text{N}_2\text{O}_4$ requires 300.30. Calculated for $\text{C}_{16}\text{H}_{16}\text{N}_2\text{O}_4 \cdot 0.25\text{H}_2\text{O}$: C, 63.04; H, 5.46; N, 9.19. Found: C, 62.91; H, 5.18; N, 9.17.

5,5'-Bis(2-carbophenoxyethyl)-2,2'-bipyridine (6). **5** (0.195 g, 0.649 mmol) and phenol (0.306 g, 3.246 mmol) in dry CH_2Cl_2 (10 mL) were cooled in ice before the addition of 1-(3-(dimethylamino)propyl)-3-ethylcarbodiimide hydrochloride (EDC) (0.435 g, 2.27 mmol) and 4-(dimethylamino)pyridine (DMAP) (8 mg, 0.0649 mmol). After the mixture stirred for 18 h at room temperature, the organic layer was washed with 1 M HCl (5 mL), 1 M NaOH (10 mL), and water (2 \times 10 mL). The CH_2Cl_2 solution was dried (Na_2SO_4), filtered, and evaporated. The crude product was purified by flash chromatography on silica gel (2 cm \times 15 cm) eluting with 1.5% methanol in CH_2Cl_2 to give the title compound as a white solid (0.215 g, 73%): $R_f = 0.3$ (5% methanol in CH_2Cl_2); mp 153.5–155 °C; ^1H NMR (250 MHz, CDCl_3) δ 2.94 (4H, t, $J = 8$ Hz, $-\text{CH}_2-$), 3.14 (4H, t, $J = 8$ Hz, $-\text{CH}_2-$), 7.03 (4H, d, $J = 8$ Hz, *o*-phenol H), 7.22 (2H, m, *p*-phenol H), 7.36 (4H, m, *m*-phenol H), 7.74 (2H, dd, $J = 8, 2$ Hz, 4-pyridine H), 8.34 (2H, d, $J = 8$ Hz, 3-pyridine H), 8.61 (2H, d, $J = 2$ Hz, 6-pyridine H); ^{13}C NMR (62.9 MHz, CDCl_3) δ 27.9, 35.5, 120.8, 121.5, 126.0, 129, 135.6, 137.0, 149.3, 150.5, 154.5, 170.9; FAB^+ MS $m/z = 453$, $\text{C}_{28}\text{H}_{24}\text{N}_2\text{O}_4$ requires 452.29. Calculated for $\text{C}_{28}\text{H}_{24}\text{N}_2\text{O}_4$: C, 74.32; H, 5.35; N, 6.19. Found: C, 73.7; H, 5.3; N, 6.5.

General Procedure for the Preparation of Iron(II) Complexes.

To a solution of the iron(II) salt with the required counterion ($\text{Fe}(\text{ClO}_4)_2 \cdot 6\text{H}_2\text{O}$ or $\text{FeCl}_2 \cdot 4\text{H}_2\text{O}$) (0.033 mmol) in the relevant solvent (5% methanol in CH_2Cl_2 for ClO_4^- salts, methanol for Cl^- salts) was added ligand **4** or ligand **6** (1 mmol). After stirring for 30 min, the solvent was removed in vacuo to give a quantitative yield of the product as a deep-red solid.

Tris(5,5'-bis(2-carbophenoxyethyl)-2,2'-bipyridine)iron(II) Perchlorate and Chloride Salts ($\text{Fe}^{\text{II}}_3(\text{ClO}_4)_2$ and $\text{Fe}^{\text{II}}_3\text{Cl}_2$). $\text{Fe}^{\text{II}}_3(\text{ClO}_4)_2$: ^1H NMR (250 MHz, $\text{MeCN}-d_3$) δ 2.67 (24H, m, $-\text{CH}_2\text{CH}_2-$), 6.88 (12H, d, $J = 8$ Hz, *o*-phenol H), 7.16 (6H, d, $J = 1.5$ Hz, 6-pyridine H), 7.25–7.43 (m, 18H, *m*- and *p*-phenol H), 7.81 (6H, dd, $J = 8, 1.5$ Hz, 4-pyridine H), 8.05 (6H, d, $J = 8$ Hz, 3-pyridine H); ^{13}C NMR (250 MHz, CDCl_3) δ 27.3, 33.7, 121.5, 123.1, 125.9, 129.4,

138.3, 140.0, 150.4, 154.2, 156.9, 170.5; FAB^+ MS $m/z = 1513$ (15, $[\text{M} - \text{ClO}_4]^+$), 1414 (70, $[\text{M} - 2\text{ClO}_4]^+$), 960 (100, $[\text{M} - \text{bipy}]^{2+}$).

$\text{Fe}^{\text{II}}_3\text{Cl}_2$: mp ca. 180 °C; ES^+ MS $m/z = 706$ (100, $[\text{M} - 2\text{Cl}]^{2+}$); ^1H NMR (250 MHz, CD_3OD) δ 2.63 (24H, m, $-\text{CH}_2\text{CH}_2-$), 6.87 (12H, d, $J = 7.5$ Hz, *o*-phenol H), 7.24 (6H, d, $J = 1.5$ Hz, 6-pyridine H), 7.31 (6H, m, *p*-phenol H), 7.42 (12H, m, *m*-phenol H), 7.81 (6H, dd, $J = 8, 1.5$ Hz, 4-pyridine H), 8.04 (6H, d, $J = 8$ Hz, 3-pyridine H); λ_{max} (ϵ) 255.6 (39 500), 265.7 (35 100), 304.3 (76 400), 394.0 (3100), 490.0 (7000), 518.3 (8100). Calculated for $\text{C}_{84}\text{H}_{72}\text{N}_6\text{O}_{12}\text{FeCl}_2 \cdot 2\text{H}_2\text{O}$: C, 66.36; H, 5.04; N, 5.53; Cl, 4.66. Found: C, 66.35; H, 5.03; N, 5.46; Cl, 4.96.

Tris(5,5'-bis(2-carbomethoxyethyl)-2,2'-bipyridine)iron(II) Perchlorate and Chloride Salts ($\text{Fe}^{\text{II}}_3(\text{ClO}_4)_2$ and $\text{Fe}^{\text{II}}_3\text{Cl}_2$). $\text{Fe}^{\text{II}}_3(\text{ClO}_4)_2$: mp 112–115 °C; ^1H NMR (250 MHz, $\text{MeCN}-d_3$) δ 1.08 (18H, t, $J = 7$ Hz, $-\text{CH}_3$), 2.45 and 2.73 (24H, br, $-\text{CH}_2\text{CH}_2-$), 3.90 (12H, m, $-\text{OCH}_2-$), 7.15 (6H, d, $J = 1.5$ Hz, 6-pyridine H), 7.93 (6H, dd, $J = 8, 1.5$ Hz, 4-pyridine H), 8.37 (6H, d, $J = 8$ Hz, 3-pyridine H); FAB^+ MS $m/z = 1223$ (3, $[\text{M} - \text{ClO}_4]^+$), 1125 (20, $[\text{M} - 2\text{ClO}_4]^+$), 562 (100, $[\text{M} - 2\text{ClO}_4]^{2+}$).

Calculated for $\text{C}_{60}\text{H}_{72}\text{N}_6\text{O}_{20}\text{FeCl}_2$: C, 54.43; H, 5.48; N, 6.35; Cl, 5.36. Found: C, 54.32; H, 5.52; N, 6.51; Cl, 5.65.

$\text{Fe}^{\text{II}}_3\text{Cl}_2$: mp 105–106 °C; ES^+ MS $m/z = 562$ (100, $[\text{M} - 2\text{Cl}]^{2+}$); ^1H NMR (250 MHz, CD_3OD) δ 1.11 (18H, t, $J = 7$ Hz, $-\text{CH}_3$), 2.58 and 2.78 (2 \times 12H, 2t, $J = 6.5$ Hz, $-\text{CH}_2\text{CH}_2-$), 3.94 (12H, 2q, $J = 7$ Hz, $-\text{OCH}_2-$), 7.30 (6H, d, $J = 1.5$ Hz, 6-pyridine H), 8.05 (6H, dd, $J = 8, 1.5$ Hz, 4-pyridine H), 8.60 (6H, d, $J = 8$ Hz, 3-pyridine H); ^{13}C NMR (62.9 MHz, CD_3OD) δ 14.5, 28.6, 34.8, 61.6, 124.6, 139.9, 142.2, 155.2, 158.9, 173.5; λ_{max} (ϵ) 254.8 (30 700), 267.1 (25 700), 304.6 (62 800), 354.5 (3000), 490.0 (4200), 520.0 (5200).

Tris(5,5'-bis(2-carboxyethyl)-2,2'-bipyridine)ruthenium(II) Hexafluorophosphate ($\text{Ru}^{\text{II}}_3(\text{PF}_6)_2$). Dried ruthenium trichloride (0.194 g, 0.935 mmol) and **4** (1.000 g, 2.806 mmol) were heated at reflux in ethylene glycol (6 mL) for 45 min. After the addition of NH_4PF_6 (0.610 g, 3.74 mmol) in water (6 mL), the solution was refrigerated overnight and the crystals that separated were removed by filtration and washed well with water before being suspended in water (10 mL). Sodium hydroxide (0.822 g, 20.55 mmol) was added and the mixture heated at reflux for 45 min until the solid dissolved to give a clear red solution. After the mixture cooled, 36% HCl (2.2 mL, 25 mmol) and NH_4PF_6 (1.5 g, 9.20 mmol) were added and the solution returned briefly to reflux. The crystals that separated upon cooling were removed by filtration, washed well with water, and dried in vacuo at 60 °C to give the title compound as a bright-orange solid (0.931 g, 77%): mp 122–125 °C; ^1H NMR (250 MHz, acetone- d_6) δ 2.61 and 2.81 (2 \times 12H, 2m, $-\text{CH}_2\text{CH}_2-$), 7.78 (6H, d, $J = 1.5$ Hz, 6-pyridine H), 8.09 (6H, dd, $J = 8, 1.5$ Hz, 4-pyridine H), 8.63 (6H, d, $J = 8$ Hz, 3-pyridine H); ^{13}C NMR (62.9 MHz, acetone- d_6) δ 28.2, 34.3, 124.6, 138.6, 142.0, 151.9, 156.2, 174.2; FAB^+ MS $m/z = 1147$ (15, $[\text{M} - \text{PF}_6]^+$), 1001 (100, $[\text{M} - 2\text{PF}_6]^+$); $v = 1706$ cm^{-1} ($\text{C}=\text{O}$); λ_{max} (ϵ) 256.8 (28 000), 294.3 (78 000), 453.2 (13 000). Calculated for $\text{C}_{48}\text{H}_{48}\text{N}_6\text{O}_{12}\text{RuP}_2\text{F}_{12} \cdot 3\text{H}_2\text{O}$: C, 42.83; H, 4.04; N, 6.24. Found: C, 42.82; H, 3.73; N, 6.40.

Tris(5,5'-bis(2-carbophenoxyethyl)-2,2'-bipyridine)ruthenium(II) Hexafluorophosphate ($\text{Ru}^{\text{II}}_3(\text{PF}_6)_2$). Phenol (87.4 mg, 0.929 mmol) and $\text{Ru}^{\text{II}}_3(\text{PF}_6)_2$ (0.100 g, 0.077 mmol) were cooled to 0 °C in dry CH_2Cl_2 (15 mL) before the addition of DMAP (9.5 mg, 0.077 mmol) and EDC (89.0 mg, 0.464 mmol). After stirring for 48 h, the CH_2Cl_2 solution was washed with 1 M HCl (2 \times 15 mL), 1 M NaOH (2 \times 15 mL), and water (15 mL). The solution was then stirred vigorously with a saturated aqueous solution of NH_4PF_6 (1 mL) for 5 h before the CH_2Cl_2 layer was separated, washed with water (15 mL), dried (Na_2SO_4), filtered, and evaporated. Flash chromatography on silica gel (20 cm \times 1.5 cm) eluting with 2.5% methanol in CH_2Cl_2 gave the title compound as an orange solid (94 mg, 70%): $R_f = 0.60$ (5% methanol in CH_2Cl_2); mp 175–176 °C; ^1H NMR (250 MHz, CDCl_3) δ 2.69 (24H, br, $\text{ArCH}_2\text{CH}_2\text{CO}_2\text{Ph}$), 6.88 (12H, d, $J = 8$ Hz, *o*-phenol H), 7.24 (6H, m, *p*-phenol H), 7.35 (12H, m, *m*-phenol H), 7.53 (6H, d, $J = 1.5$ Hz, 6-pyridine H), 7.55 (6H, dd, $J = 8, 1.5$ Hz, 4-pyridine H), 7.73 (6H, d, $J = 8$ Hz, 3-pyridine H); ^{13}C NMR (62.9 MHz, 5% $\text{CD}_3\text{OD}/\text{CDCl}_3$) δ 27.0, 33.6, 121.4, 123.4, 126.0, 129.4, 137.4, 140.4, 150.4, 151.2, 154.7, 170.6; FAB^+ MS $m/z = 1603$ (100,

[M - PF₆]⁺), 1459 (45, [M - 2PF₆]⁺). Calculated for C₈₄H₇₂N₆O₁₂-RuP₂F₁₂: C, 57.70; H, 4.15; N, 4.81. Found: C, 57.94; H, 4.42; N, 5.24.

Tris(5,5'-bis(2-carboxypentoxethyl)-2,2'-bipyridine)ruthenium-(II) Hexafluorophosphate (Ru^{II}7₃ (PF₆)₂). Ru^{II}7₃ (PF₆)₂ was prepared using an identical procedure to that for Ru^{II}6₃ (PF₆)₂ but substituting *n*-pentanol (0.450 g, 5.04 mmol) in place of phenol. The product was purified by flash chromatography on silica gel (20 cm × 1.5 cm) eluting with 2% methanol in CH₂Cl₂ to give the title compound as a hygroscopic orange solid (62 mg, 47%): *R*_f = 0.3 (5% methanol in CH₂Cl₂); ¹H NMR (250 MHz, CDCl₃) δ 0.86 (30H, m, -CH₂CH₃), 1.43 (12H, m, -OCH₂CH₂CH₂-), 1.61 (12H, m, OCH₂CH₂-), 2.54 and 2.83 (2 × 12H, 2m, ArCH₂CH₂CO₂R), 3.93 (12H, m, -OCH₂-), 7.54 (6H, d, *J* = 1.5 Hz, 6-pyridine H), 7.81 (6H, dd, *J* = 8, 1.5 Hz, 4-pyridine H), 8.34 (6H, d, *J* = 8 Hz, 3-pyridine H); FAB⁺ MS *m/z* = 1566 (100, [M - PF₆]⁺), 1423 (75, [M - 2PF₆]⁺), [M - PF₆]⁺ requires 1567.6711, found *m/z* = 1567.6863; λ_{max} (ε) 265.4 (35 000), 295.5 (93 000), 453.9 (16 000).

cis-Dichlorobis(5,5'-dimethyl-2,2'-bipyridine)ruthenium(II) (Ru^{II}1₂·Cl₂). **1** (1.417 g, 7.69 mmol), RuCl₃·3H₂O (1.000 g, 3.82 mmol), and lithium chloride (1.100 g, 25.9 mmol) were heated at reflux in HPLC grade DMF (8 mL) for 7 h. The resulting solution was poured into acetone (25 mL), and after refrigeration overnight the precipitate was removed by filtration and washed with water (3 × 25 mL) and diethyl ether (3 × 25 mL) before being dried in vacuo to yield the title compound as a black solid (1.72 g, 83%) which was used directly in the next step.

Bis(5,5'-dimethyl-2,2'-bipyridine)(5,5'-bis(2-carboxyethyl)-2,2'-bipyridine)ruthenium(II) Hexafluorophosphate (Ru^{II}1₂·4 (PF₆)₂). A solution of crude Ru^{II}1₂·Cl₂ (0.500 g, 0.868 mmol) and **4** (0.340 g, 0.955 mmol) in 50% ethanol/water (20 mL) was heated at reflux for 3 h. After the mixture cooled, a solution of NH₄PF₆ (1.4 g) in water (20 mL) was added with the formation of an orange precipitate which was extracted into CH₂Cl₂ (50 mL). The CH₂Cl₂ layer was separated and washed with 1 M HCl (2 × 25 mL), 1 M NaOH (2 × 25 mL), and water (25 mL) before being dried (Na₂SO₄), filtered, and evaporated. The product was purified by flash chromatography on silica gel (2 cm × 35 cm) eluting with 2% methanol/CH₂Cl₂, collecting the fast-running band to give the title compound as an orange solid (0.702 g, 72%): *R*_f = 0.70 (10% methanol in CH₂Cl₂); mp ca. 120 °C; ¹H NMR (250 MHz, acetone-*d*₆) δ 1.10 (6H, t, *J* = 8 Hz, -OCH₂CH₃), 2.21 (2 × 6H, 2s, ArCH₃), 2.57 and 2.82 (2 × 4H, 2m, ArCH₂CH₂CO₂Et), 3.95 (4H, m, OCH₂CH₃), 7.61, 7.80, and 7.85 (3 × 2H, 3d, *J* = 1.5 Hz, 6-pyridine H), 7.95–8.09 (6H, m, 4-pyridine H), 8.62 (6H, m, 3-pyridine H); ¹³C NMR (62.9 MHz, acetone-*d*₆) δ 14.4, 18.4, 28.1, 34.5, 60.9, 124.2, 124.3, 124.4, 138.6, 139.3, 139.0, 152.0, 152.1, 152.5, 155.7, 155.8, 156.1, 172.4; FAB⁺ MS *m/z* = 971 (100, [M - PF₆]⁺), 826 (75, [M - 2PF₆]⁺), 413 (86, [M - 2PF₆]²⁺); λ_{max} (ε) 265.0 (63 000), 294.1 (140 000), 446.4 (25 000). Calculated for C₄₄H₄₈N₆O₄RuP₂F₁₂: C, 47.34; H, 4.34; N, 7.53; Found: C, 47.6; H, 4.3; N, 7.8.

Bis(5,5'-dimethyl-2,2'-bipyridine)(5,5'-bis(2-carboxyethyl)-2,2'-bipyridine)ruthenium(II) Hexafluorophosphate (Ru^{II}1₂·5 (PF₆)₂). Ru^{II}1₂·4 (PF₆)₂ (0.112 g, 0.100 mmol) and sodium hydroxide (0.206 g, 5.15 mmol) in water (5 mL) were heated at reflux for 2.5 h. The solution was cooled before the addition of 36% HCl (0.608 g, 6 mmol) and NH₄PF₆ (1.00 g) and then briefly returned to reflux. After cooling, the suspension was extracted with CH₂Cl₂ (4 × 15 mL), and the combined CH₂Cl₂ extracts were washed with water, dried (Na₂SO₄), filtered, and evaporated to give the title compound as a bright-orange solid (0.102 g, 96%): *R*_f = 0.0 (10% methanol/CH₂Cl₂); mp 188–192 °C; ¹H NMR (250 MHz, acetone-*d*₆) δ 2.20 (2 × 6H, 2s, -CH₃), 2.57 and 2.83 (2 × 4H, 2m, ArCH₂CH₂COOH), 7.67, 7.80, and 7.87 (3 × 2H, 3d, *J* = 1.5 Hz, 6-pyridine H), 7.98 and 8.09 (4H and 2H, 2m, 4-pyridine H), 8.62 (6H, m, 3-pyridine H); ¹³C NMR (62.9 MHz, acetone-*d*₆) δ 18.5, 28.1, 34.2, 124.3, 124.5, 138.7, 139.1, 139.2, 139.3, 142.1, 152.0, 152.1, 152.3, 155.8, 156.1, 173.3; FAB⁺ MS *m/z* = 915 (85, [M - PF₆]⁺), 769 (100, [M - 2PF₆]⁺), 385 (30, [M - 2PF₆]²⁺). Calculated for C₄₀H₄₀N₆O₄RuP₂F₁₂: C, 45.33; H, 3.80; N, 7.93; Found: C, 44.8; H, 4.1; N, 7.9.

Bis(5,5'-dimethyl-2,2'-bipyridine)(5,5'-bis(2-carboxyphenoxethyl)-2,2'-bipyridine)ruthenium(II) hexafluorophosphate (Ru^{II}1₂·6 (PF₆)₂). To a solution of Ru^{II}1₂·5 (PF₆)₂ (50.9 mg, 0.048 mmol), phenol (45.0 mg, 0.478 mmol), and DMAP (0.5 mg) in CH₂Cl₂ (2 mL) at 0 °C was added EDC (36.8 mg, 0.192 mmol) in one portion. The mixture was stirred at room temperature for 18 h before dilution with CH₂Cl₂ (10 mL) and washing with 1 M HCl (10 mL), 1 M NaOH (10 mL), and water (10 mL). After drying (Na₂SO₄), the solvent was removed in vacuo and the crude product purified by flash chromatography on silica gel (1 cm × 15 cm) eluting with 2% methanol in CH₂Cl₂ to give the title compound as an orange solid (44.5 mg, 75%): mp ca. 150 °C; ¹H NMR (250 MHz, acetone-*d*₆) δ 2.09 and 2.13 (2 × 6H, 2s, -CH₃), 2.92 (8H, br, -CH₂CH₂-), 6.95 (4H, d, *J* = 8 Hz, *o*-phenol H), 7.27 (2H, t, *J* = 8 Hz, *p*-phenol H), 7.41 (4H, t, *J* = 8 Hz, *m*-phenol H), 7.70, 7.75, and 7.93 (3 × 2H, 3s, *J* = 1.5 Hz, 6-pyridine H), 7.88 and 7.95 (2 × 2H, 2dd, *J* = 8, 1.5 Hz, 4- and 4'-dimethylbipy H), 8.15 (2H, dd, *J* = 8, 1.5 Hz, 4-pyridine H), 8.43 and 8.51 (2 × 2H, 2d, *J* = 8 Hz, 3- and 3'-dimethylbipy H), 8.69 (2H, d, *J* = 8 Hz, 3-bipyridine H); ¹³C NMR (62.9 MHz, acetone-*d*₆) δ 18.4, 28.0, 34.5, 122.4, 124.2, 124.3, 124.6, 126.7, 130.3, 138.7, 139.2, 139.3, 139.0, 139.1, 151.7, 151.9, 152.6, 155.8, 156.3, 171.3; FAB⁺ MS *m/z* = 1068 (98, [M - PF₆]⁺), 922 (100, [M - 2PF₆]⁺); λ_{max} (ε) 265.4 (38 000), 295.5 (99 000), 447.2 (16 000). Calculated for C₅₄H₄₈N₆O₄RuP₂F₁₂·3H₂O: C, 50.27; H, 4.22; N, 6.51; Found: C, 49.94; H, 4.20; N, 6.56.

Acknowledgment. We thank the Lister Institute (C.A.H.), the EPSRC, and Zeneca Pharmaceuticals (P.C.M.) for financial support and Dr. J. A. Thomas for useful discussions.

JA973938+